Food and Chemical Toxicology 125 (2019) 333–340

Contents lists available at ScienceDirect

Food and Chemical Toxicology

journal homepage: www.elsevier.com/locate/foodchemtox

Ameliorative effect of salidroside from *Rhodiola Rosea* L. on the gut microbiota subject to furan-induced liver injury in a mouse model

Yuan Yuan, Xuan Wu, Xu Zhang, Yilin Hong, Haiyang Yan*

College of Food Science and Engineering, Jilin University, 130062 Changchun, China

ARTICLE INFO

Keywords:
Furan
Salidroside
Gut microbiota
Liver injury

ABSTRACT

In our study, the ameliorative effect of salidroside (SAL) from *Rhodiola Rosea* L. on the intestinal microflora subject to furan-induced liver injury in a mouse model was investigated by 16 S rDNA, oxidative indexes, LPS and cytokine levels. The results demonstrated that SAL alleviated hepatic oxidative injury by inhibiting the activities of AST, ALT and the content of MDA, and promoting the activities of SOD, GSH and GST, compared to the furan-treated group. SAL significantly modified the intestinal microbial diversity and downregulated the circulating levels of serum LPS, IL-6, and TNF-α, as well as enhanced the content of IL-10. Importantly, SAL dramatically increased LPS-suppressing bacteria genera *Akkermansia,* and decreased LPS-producing bacteria phyla *Proteobacteria*. Our results indicate that SAL supplement restrains intestinal microbial dysbiosis and systemic low-grade inflammation induced by furan. Hopefully, SAL is a potential therapeutical and prophylactic compound in medicament for hepatic diseases.

1. Introduction

Furan has been considered as a possible human carcinogen (Group 2B) by the International Agency for Research on Cancer (IARC) (Zuckerman, 1995). With thermal food processing, the Maillard reaction (Condurso et al., 2018), lipid oxidation, thermal degradation of sugars (Crews and Castle, 2007) and mutual reactions between degradation products result in the formation of furan (Maga, 1979). Furan has been detected in different types of food, including coffee, baby food and soups (Crews and Castle, 2007). Mainstream cigarette smoke contains up to 65 mg furan per cigarette (Smith et al., 2000). Some novel food processing technologies are likely to induce the formation of furan as well. Up to 23.6 ng/mL and 60 ng/mL furan were detected in UV-treated apple cider and orange juice (Hu et al., 2016), respectively. *In vitro* and *in vivo* toxicity of furan has been investigated. A 3-month research investigating the impact of intragastrically administered furan on liver and kidney in rats by biochemical, morphological, histopathological and histomorphometrical inspections revealed that furan exerted adverse influences on the two organs (Selmanoğlu et al., 2012). As a typical food contaminant and even a cancerogen, furan primarily targets liver. Based on previous achievements, more efforts are needed to investigate furan formation and its toxicity mechanism.

Salidroside (SAL) is a phenolic glycoside compound in Rhodiola plants, and has long been utilized as an important ingredient in functional foods. Its anti-inflammatory, anti-aging, antioxidant and hepatoprotective effects have been firmly confirmed (Endale et al., 2013; X et al., 2013). The neuroprotective effect of SAL against ß-amyloid-induced oxidative stress in SH-SY5Y human neuroblastoma cells was explored (Zhang et al., 2010). SAL has been demonstrated to function in alleviating liver injury (Yang et al., 2016; Zou et al., 2015), which encouraged our interest in the current study.

Recent studies revealed the roles of the gut-liver axis in liver injury. Gut microbiota acts a vital part in the mechanism of liver injury, as has been elucidated. Gut microbiota is closely related to the pathogenesis and progression of fatty liver, non-alcoholic steatohepatitis (NASH), fibrosis, and cirrhosis (De et al., 2014). Gut microbiota affects immunity in intestine (Walker et al., 2011), and leads to inflammation of intestinal surrounding tissues as well.

16 S rDNA sequencing has been extensively used to uncover the evolving influence of gut microbiota. Multiple paragenetic intestinal bacteria have a lasting impact on immunity and metabolism through interactions of microbial cell components with gene products including lipopolysaccharides (LPS), peptidoglycan, and flagellin (Clemente et al., 2012). Studies revealed that intestinal microbiota dysbiosis significantly influenced liver metabolism, probably owing to the incremental metabolism of toxic bacteria, and biggish gut permeability. The dysbiosis could bring about higher levels of LPS in systemic revolution, and ultimately a low-grade systemic inflammatory status (Chang et al.,

* Corresponding author. College of Food Science and Engineering, Jilin University, Changchun, 130062, China.
E-mail address: yanhyjlu@163.com (H. Yan).

https://doi.org/10.1016/j.fct.2019.01.007
Received 22 September 2018; Received in revised form 8 January 2019; Accepted 10 January 2019
Available online 14 January 2019

2015).

Our previous studies proved the ameliorative influences of SAL settlement against furan-induced liver injury by determining the corresponding biochemical indexes (Yuan et al., 2013). The achievements stimulated our interest in investigating the influence of SAL on the intestinal microflora subject to liver injury induced by furan. However, limited studies have been found on the effect of SAL on the intestinal microflora subject to furan-induced liver in mouse models. Hopefully, SAL might contribute to alleviating liver injury by irritating the abundance and activity of particular gut bacteria. In the current study, we pioneeringly investigated how SAL regulated the community structure, composition, and metabolites of gut microbiota by 16 S rDNA sequencing, as well as its therapeutic effects on systemic low-grade inflammation in furan-induced mice.

2. Materials and methods

2.1. Materials

Furan (CAS: 110-00-9, 99.5%) was purchased from Chem Service (Pennsylvania, USA) and SAL (CAS: 10338-51-9, 98%) was obtained from Shanghai Yuanye Bio-Technology Co., LTD (Shanghai, China). Male Balb/c mice were purchased from Liaoning ChangSheng Biotechnology Co. LTD (Benxi, China). ALT, AST, GSH, GST, SOD and MDA were purchased from Nanjing Jiancheng Bioengineering Institute (Nanjing, China). IL-6, IL-10, as well as TNF-α Elisa kit were purchased from ThermoFisher Scientific (Shanghai, China). ELISA Kit for LPS was purchased from GenScript USA Inc. (Nanjing, China). DNA extraction kit was purchased from Omega Bio-tek USA, Inc. All other chemicals and reagents were of analytical grade.

2.2. Experimental animals

The experiments were implemented in conformity to the Guideline for Animal Experimentation of Jilin University (Changchun, China). The protocol for animals involved in our research was granted by the Ethical Welfare Committee of Jilin University (No. 20171010). Specific pathogen-free male Balb/c mice weighing 20–22 g were maintained in an air-conditioned room at 20–24 °C and 20–40% relative moisture capacity with independent access to food and water. After a one-week acclimatization period, mice were separated into five groups (5–6 mice per cage). Furan was dissolved in corn oil to the concentration of 0.8 mg/mL. SAL was diluted in normal saline to reach the final concentration of 1, 2 and 4 mg/mL, respectively. The dose volume was dependent on the BW of each mouse. One group was conventionally oral gavage with corn oil as the control group (marked as CON group), and the other four groups were gavaged with furan for 30 days (marked as FUR 8 and SAL group). From day 16, SAL (10, 20, and 40 mg/kg/day) was daily intragastrically administered, marked as SAL 10, SAL 20 and SAL 40, respectively.

Mice were fasted for 12 h and anesthetized with 10% chloral hydrate prior to sampling. Blood was sampled from the eyes and stored at 22 ± 2 °C for 4 h; serum was separated by centrifugation at 1259 × *g* at 4 °C for 10 min. Livers were removed and washed entirely with ice-cold normal saline. The tissues were homogenized with 0.9% normal saline using a tissue homogenizer and centrifuged at 1259 × *g* at 4 °C for 10 min. The supernatant was applied to biochemical analysis. The cecum of the mice was immediately excised and the contents were collected for DNA extraction.

2.3. Biochemical analyses

Activities of AST, ALT, GSH, GST, SOD and MDA content were determined using commercial kits on the basis of the manufacturer's instructions. TNF-α, IL-10 and IL-6 were detected by commercial ELISA kits in accordance with the user guide. The LPS level was examined by Chromogenic LAL Endotoxin Assay Kit, based on the user guide.

2.4. DNA extraction and PCR amplification

DNA from the content of cecum was obtained by the E.Z.N.A.® Stool DNA Kit on the basis of the user guide. The entire DNA was eluted in 50 μL of Elution buffer and deposited at −80 °C before PCR by LC-Bio Technology Co., Ltd (Hang Zhou, China). The V4 region of the procaryotic small-subunit (16 S) rDNA gene was magnified with slightly modified versions of primers 515F (5′-GTGYCAGCMGCCGCGGTAA-3′) and 806R (5′-GGACTACHVGGGTWTCTAAT-3′) (Walters et al., 2016). The 5′ ends of the primers were labeled with particular barcods per sample and sequencing general duty primers. PCR amplification was carried out in a cumulative volume of 25 μL reaction mixture. The PCR products were purified by AMPure XT beads (Beckman Coulter Genomics, Danvers, MA, USA) and quantified by Qubit (Invitrogen, USA). The libraries were sequenced on 250 PE MiSeq runs and one library was sequenced with both protocols using the standard Illumina sequencing primers.

2.5. Intestinal microbiota analysis

Samples were sequenced on an Illumina MiSeq platform on the basis of user guide, supplied by LC-Bio Technology Co., Ltd (Hang Zhou, China). The diversities of the predominant species in different groups and Multiple Sequence Alignment were implemented by the PyNAST software to analyze phylogenetic connection of diverse OTUs. Alpha diversity was used to analyze species complexity according to 4 indices, including Chao1, Shannon, Simpson and Observed species. Each indice was computed with QIIME (Version 1.8.0). Beta diversity was computed by principle co-ordinates analysis (PCoA) and cluster analysis by the QIIME software (Version 1.8.0). The linear discriminant analysis (LDA) effect size (LEfSe) method was employed to identify the biomarker discovery, which highlights statistical significance as well as biological relevance.

2.6. Statistical analysis

All statistical analyses were implemented through the SPSS 19.0.0 software (IBM Corporation, Somers, NY, USA) and R 3.3.2 software. The significance of difference was computed by one-way ANOVA test, and the results with $p < 0.05$ were regarded as statistically significant. Other quantitative data were reported using the mean ± standard deviation. The graphs were described through the OriginPro 8.5 software (OriginLab Corporation, Northampton, MA, USA).

3. Results

3.1. SAL alleviates liver injury induced by furan

In order to investigate the effect of SAL on liver injury induced by furan, the levels of biochemical indexes in serum and liver tissue homogenates were tested. AST and ALT levels in FUR 8 were apparently higher than those of the CON group ($p < 0.05$; Table 1). With SAL concentration increasing, AST and ALT activities gradually decreased. The activities of AST and ALT were reduced by 48.03%, and 58.90% in the SAL 40 group, respectively. Furan caused a marked decline in GSH and GST activities compared to the CON group ($p < 0.05$; Table 1). GSH and GST activities, however, were found significantly enhanced in the groups treated with SAL, compared to the FUR 8 group ($p < 0.05$). GST activity was significantly improved by 94.39% after SAL treatment at 40 mg/kg/day. The changes of SOD, MDA in the liver of furan-induced mice were showed in Table 1. SOD activity of furan-induced mice significantly decreased by 64.45%, compared to the CON group. SOD activity in mice livers was higher with increasing SAL at all concentrations. The same tendency of MDA was observed.

Table 1
Effects of SAL on the activities of ALT, AST in the serum and GSH, GST, SOD, MDA in the liver of furan-treated mice.[a].

	AST (U/L)	ALT (U/L)	GSH (nmol/mg)	GST (U/mgprot)	SOD (U/mgprot)	MDA (nnol/mgprot)
CON group	12.66 ± 0.56a	9.68 ± 1.18a	21.11 ± 0.84a	65.4 ± 0.36a	355.5 ± 5.54a	0.30 ± 0.16a
FUR 8 group	31.46 ± 4.03b	28.32 ± 0.46b	11.92 ± 2.73b	26.03 ± 2.77b	126.4 ± 6.67b	0.70 ± 0.28b
SAL 10 group	25.38 ± 2.23c	25.13 ± 2.03b	11.97 ± 1.67b	46.02 ± 1.21b	211.8 ± 7.85c	0.60 ± 0.01c
SAL 20 group	18.76 ± 1.62c	18.60 ± 3.67b	13.52 ± 0.77b	52.18 ± 0.61a	237.7 ± 6.45a	0.53 ± 0.16c
SAL 40 group	16.35 ± 0.78a	11.64 ± 1.02a	15.50 ± 1.69b	50.60 ± 1.07c	297.9 ± 4.11a	0.33 ± 0.07a

[a] Data are presented as the mean ± SD (n = 5–6). Values in the same column that do not share the same lowercase letter are significantly different ($p < 0.05$).

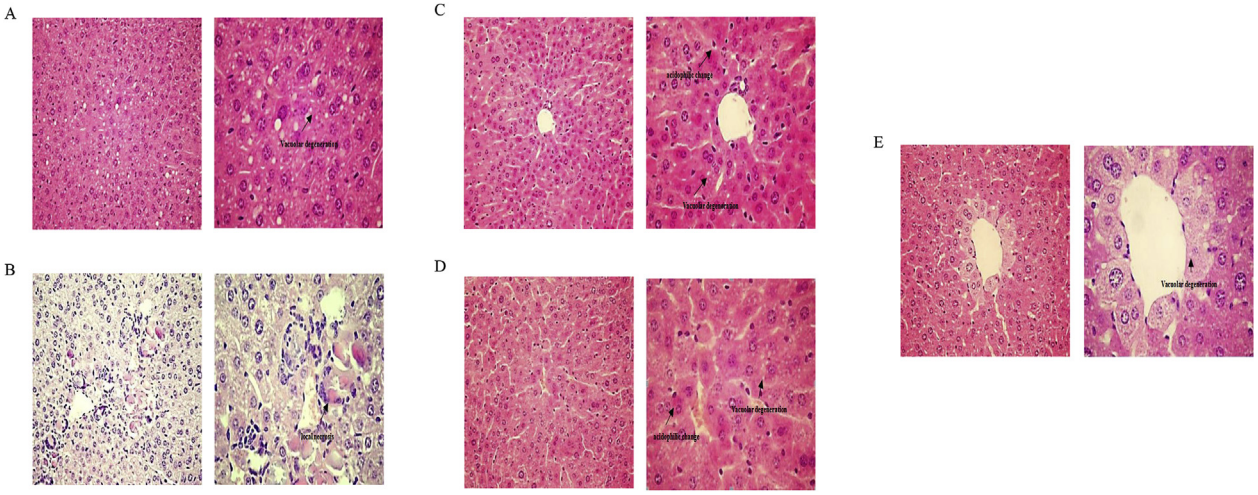

Fig. 1. Effects of SAL on the hepatic HE results of furan-treated mice. (Scale bar, 1:200, 1:400, respectively) (A) Representative HE image of CON group. (B) Representative HE image of FUR 8 group. (C–E) Representative HE image of SAL 10, 20, 40 group.

Similarly, compared with the CON group (Fig. 1A), hematoxylin-eosin staining (HE) results revealed the liver of the FUR 8 group (Fig. 1B) had significant hepatic necrosis accompanied by nuclear isotypes, which were relieved with supplemented of SAL (Fig. 1C–E). No significant difference was detected between SAL 40 and CON. These results demonstrated that SAL supplementation alleviated furan-induced local inflammation.

3.2. SAL regulates the composition of gut microbiota induced by furan

The effect of the gut microbiota composition on mice after SAL treatment was explored with 16 S rDNA sequencing using Miseq as a sequencing platform in the current study. In order to facilitate the study concerning species compositional diversity information, we clustered the valid sequences of all the above samples into OTUs on the basis of 97% sequence similarity. The rank abundance graph (Fig. 2A) proved that the majority of OTUs were displayed in low abundance in the gut microbiota. The chao1 index and observed species index mainly reflected the OTU species number, while the Shannon (Fig. 2B) and Simpson indices (Fig. 2C) were relative to the average and homogeneity. The FUR 8 group had a lower abundance and evenness index (Chao 1, 980.87; observed_species, 791.8; Shannon, 6.67; and Simpson, 0.96) than CON (Chao 1, 1028.97; observed_species, 833.17; Shannon, 6.75; and Simpson, 0.97). After the intake of SAL, the chao 1 index and other observed species indexes were increased, positively correlated with the concentration of SAL. To evaluate the degree of the comparability in terms of microbial communities among 5 groups, the beta diversity and principal co-ordinates analysis (PCoA) were performed on the basis of the unweighted UniFrac distances. PCoA displayed significant separation between the furan-treated group and the CON group (Fig. 2D), indicating a large difference in microbial composition. Despite remarkable inter-individual alterations, the microbiota from the furan-treated mouse model treated with SAL at different concentrations was obviously divided by PCoA. The value on the axis records the percentage of results interpreted by each dimension. This figure showed that PCo1 and PCo2 accounted for 14.65% and 12.40% of the overall analysis results.

At the phylum level, 10 main phyla composited the gut microbiota: *Firmicutes, Bacteroidetes*, *Proteobacteria*, *Verrucomicrobia*, *Actinobacteria*, *Candidatus*, *Saccharibacteria*, *Cyanobacteria*, *Candidatus_Melainabacteria*, *Acidobacteria*, and *Tenericutes* (Fig. 3A). SAL treatment could decrease the relative abundance of *Proteobacteria*, *Candidatus Saccharibacteria* and increased *Verrucomicrobia*, *Candidatus_Melainabacteria.* Compared with the CON group, the augment with significance in the species quantity of *Cyanobacteria* was found in the furan-treated group. However, no significant difference was detected between SAL-related concentration groups and FUR 8 ($p > 0.05$). It indicated that the intake of SAL could not inhibit the growth of *Cyanobacteria*. Surprisingly, compared with FUR 8, only *Bacteroidetes* were increased in SAL 10 and SAL 40.

In FUR 8, the most plentiful order authenticated in the gut microbiota community was *Clostridiales* (Fig. 3B). *Bacteroidales*, *Desulfovibrionales*, *Lactobacillales* and *Coriobacteriales* were of relatively low abundance. *Rhodospirillales* was the incremental bacteria at the order level after furan settlement alone, with the relative content increasing from 0.00 ± 0.02 to 0.05 ± 0.02 ($p < 0.05$). And the content of *Rhodospirillales* displayed a degressive trend, especially after 40 mg/kg/day treatment with SAL. Compared with the CON group, the relative abundance of *Pseudomonadales* was reduced and *Verrucomicrobiales* displayed an increasing tendency, but they were not significantly changed in the FUR 8 group ($p > 0.05$).

The results at the family level of the gut microbiota were achieved. *Christensenellaceae* and *Rhodospirillaceae* were significantly enhanced after furan treatment (Fig. 3C). *Christensenellaceae* was the representative species at each concentration of SAL and its abundance apparently decreased from 0.06 ± 0.02 to 0.03 ± 0.03 ($p < 0.05$)

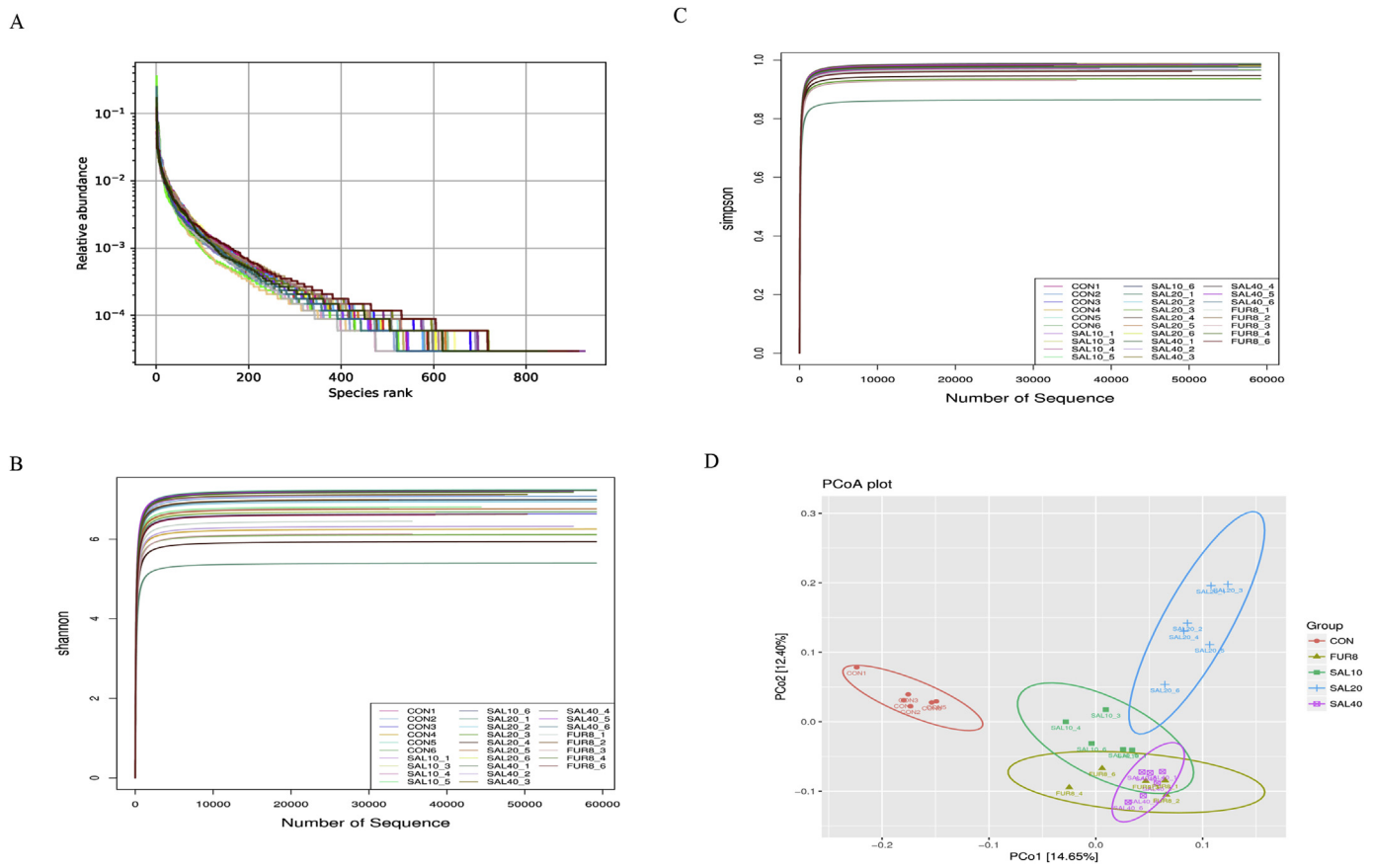

Fig. 2. Effects of SAL on the composition of gut microbiota. (A) Rank abundance curve of bacterial OTUs derived from each sample. The Shannon (B) and Simpson (C) indices were used to estimate the diversity of the gut microbiota. (D) PCoA diagram illustrating the difference in microbial composition among the samples.

after 20 mg/kg/day treatment. Interestingly, compared with the FUR 8 group, the mice administered with SAL didn't result in the abundance of *Rhodospirillaceae*, which was not consistent to the microbial changes in the order.

The heat map performed genera were displayed at different levels in each sample. More *Olsenella*, *Sporobacter*, *Anaerovorax*, *Insolitispirillum* and *Blautia* were observed clearly but the abundance of *Eisenbergiella* declined significantly after furan treatment ($p < 0.05$) from the genus-level analysis (Fig. 3D). SAL treatment led to the decline in the number of *Sporobacter, Blautia, Desulfovibrio, Anaerofustis* and *Olsenella.* The relative abundance of *Blautia* in SAL 10 declined significantly, while *Bifidobacterium* and *Vasilyevaea* showed a tendency of decline in SAL 40 ($p < 0.05$). For SAL 20, the relative abundance of *Akkermansia* and *Roseburia* was significantly enhanced over the treatment ($p < 0.05$), while these changes were not detected in other groups ($p > 0.05$).

To identify specific bacteria related to SAL supplement, we investigated the gut microbiota in the furan-induced mouse model by LEfSe. The significant discrepancies in taxa between per concentration and the identified pivotal phylotypes as microbiological markers at miscellaneous phylogenetic levels were presented in Fig. 4. The screening conditions for this analysis were $p < 0.05$ and LDA > 2.0. At the phylum level, *Candidatus_Melainabacteria* presented significant differences in SAL 20, while *Candidatus Saccharibacteria* were found markedly different in SAL 40. *Verrucomicrobia* were promoted after the supplement of 20 mg/kg/day of SAL, and *Actinobacteria* were markedly plentiful in SAL 10.

3.3. SAL decreases systemic low-grade inflammation and serum LPS induced by furan

The ameliorative effect of SAL on the systemic inflammation induced by furan is elucidated by the levels of cytokines in the serum. As shown in Fig. 5A and B, SAL supplementation significantly decreased the furan-induced high levels of IL-6 and TNF-α. Concomitantly, IL-10 level was significantly enhanced compared with FUR 8 (Fig. 5C). Administration of furan induced a markedly higher levels of IL-6 and TNF-α, and remarkable decline of IL-10 level compared to the CON group ($p < 0.05$). As a metabolite of bacteria in gut, LPS promoted the accumulation of toxic substances, and SAL treatment decreased LPS levels in serum, compared with the FUR 8 group ($p < 0.05$; Fig. 5D).

4. Discussion

Exposure to high levels of furan could induce liver injury (Bakhiya and Appel, 2010). According to our previous studies, the ameliorative effects of SAL are attributed to the competence of scavenging free radicals and improving antioxidative system (Yuan et al., 2013). And the effects were correlated with the concentrations of SAL ranging from 10 to 40 mg/kg/day. For a deeper insight into the gut-liver axis, the underlying mechanisms of the mutual effect between gut flora and liver, as well as the protective effects, deserve to be further investigated. Herein, the effects of SAL on the intestinal microflora in mice of liver injury induced by furan were investigated for the first time.

In our research, furan toxicity was presented by AST, ALT, GSH, GST and SOD activities as well as MDA content (Table 1). ALT and AST were featured in the biomarkers for early liver injury. Their increased activities in plasm showed increased permeability and necrosis of hepatocytes. GST serves as a crucial phase II enzyme and obliterates electrophilic oxidants through consuming GSH (Pabst et al., 1974). We observed a dramatic decline in GST and GSH activities in furan-induced mice, which implied that furan remarkably undermined hepatic tissue. SOD acts on evaluating the oxidative stress of an organism. Treatment

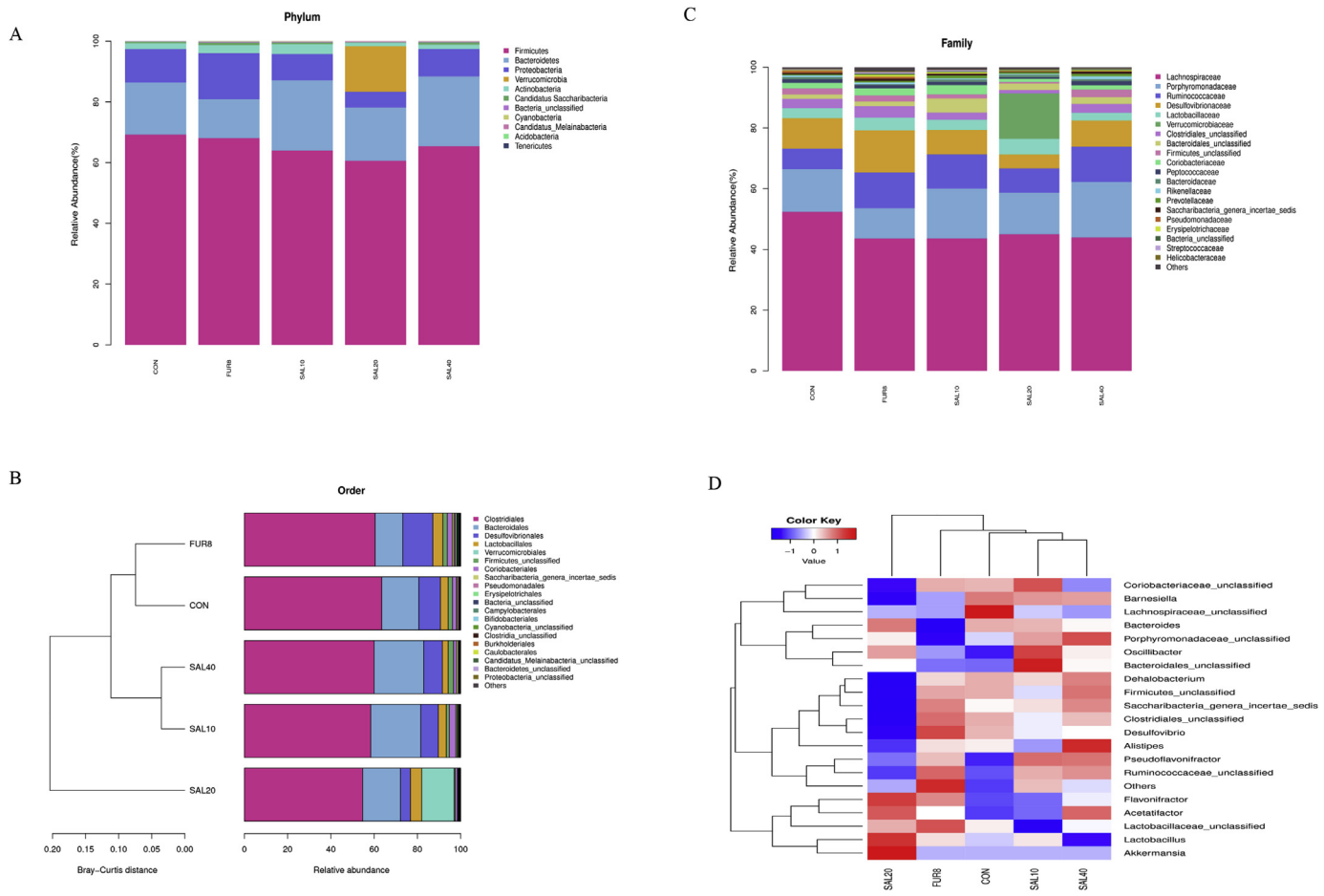

Fig. 3. Effects of SAL on the diversity of gut microbiota. The bar graph of the top phyla (A), relative abundance of the top orders (B) and the top families (C), as well as heat map of the genera with the highest frequency and relative abundance (D) from each sample.

with 8 mg/kg/day furan for 30 days dramatically reduced the activities of SOD in liver, indicating that furan induced oxidative damage. Some peroxidation researches manifested MDA worked as a biomarker of free radical-mediated lipid peroxidation injury (Cordelli et al., 2010). Relevant results showed that furan led to a conspicuous augment in MDA contents. Our results clearly confirmed that SAL was able to improve oxidative stress and repair liver injury in the furan-induced mouse model, as obvious from the variations in GST, GSH and SOD activities, and the contents of MDA. Overall, the furan-induced liver injury was alleviated by SAL.

More studies have concentrated on illuminating the relationship between intestinal microbiota and low-grade inflammation involved in metabolic diseases. Disorder of intestinal microbiota results in the modification of immune response and is concerned with various liver diseases including liver fibrosis, non-alcoholic fatty liver disease (NAFLD) (Henaomejia et al., 2012), alcoholic liver disease and hepatocellular carcinoma (HCC) (Qin et al., 2014). Accompanied with hepatic repair in furan-treated mice, supplement with SAL for 15 days caused an altered intestinal bacteria composition, which was distinct from the CON group. Consistently, PCoA plot proved the samples in FUR 8 and CON were obviously different ($p < 0.05$). Simultaneously, the samples in SAL 20 were gathering consumingly and gradually far from FUR 8, indicating that SAL regulated the communities of gut microbiota towards a representative orientation (Fig. 2D). 16 S rDNA was employed in sequencing 6 samples in each group. A remarkable increase was detected in the abundance of the *Cyanobacteria* phylum after furan administration compared with the CON group (Fig. 3A). *Cyanobacteria* produce Microcystins-LR (MC-LR), which can disorder lung and liver actions and deteriorate redox balance (Bittencourtoliveira et al., 2014; Li et al., 2017). It is generally accepted that exposure to MC-LR results in liver damage, followed by detriment to other organs such as lung, kidney and gut (Ito et al., 2001). Our results showed that furan promoted the growth of *Cyanobacteria* in gut, and the increased lipid peroxidation in mice liver resulted from the exposure to MC-LR (Jayaraj et al., 2006). Although the treatment with SAL can not significantly inhibit its growth, the proliferation of *Cyanobacteria* may serve as a potential marker for liver injury, which provides new ideas for the follow-up research. It is notable that the LPS-suppressing phyla *Verrucomicrobia* in SAL 20 was remarkably enhanced, and the LPS-producing phyla *Proteobacteria* was distinctly reduced with respect to the CON group (Fig. 3A). Coincidentally, prevenient researches also demonstrated that the overgrowth of *Proteobacteria* was related with colitis (Carvalho et al., 2012). However, some found that *Proteobacteria* could be enhanced along with the improvement of inflammation (Caesar et al., 2015). We infer that *Cyanobacteria* and *Proteobacteria* have as yet undisclosed effects in liver injury, so more explorations on them are needed.

SAL supplementation enhanced the abundance of *Olsenella, Sporobacter, Anaerovorax, Ruminococcaceae, Insolitispirillum, Blautia, Christensenellaceae* and *Desulfovibrionales.* Besides, we detected a significant increase in the abundance of *Roseburia*, *Akkermansia* in SAL 20 alone (Fig. 3D). Previous studies have revealed that LPS-producing families/genera are limited to several families/genera (*Enterobacteriaceae, Clostridium cluster XI, Prevotella, and SFB*), while *Lactobacillus*, *Bifidobacterium*, *Enterococcus faecium*, *Clostridium cluster XIVa*, *Clostridium cluster IV*, and *Akkermansia* are basically LPS-suppressing genera (Louis et al., 2010), which are associated with weakening the intestinal permeability and inflammatory (Martín et al., 2014), implementing the

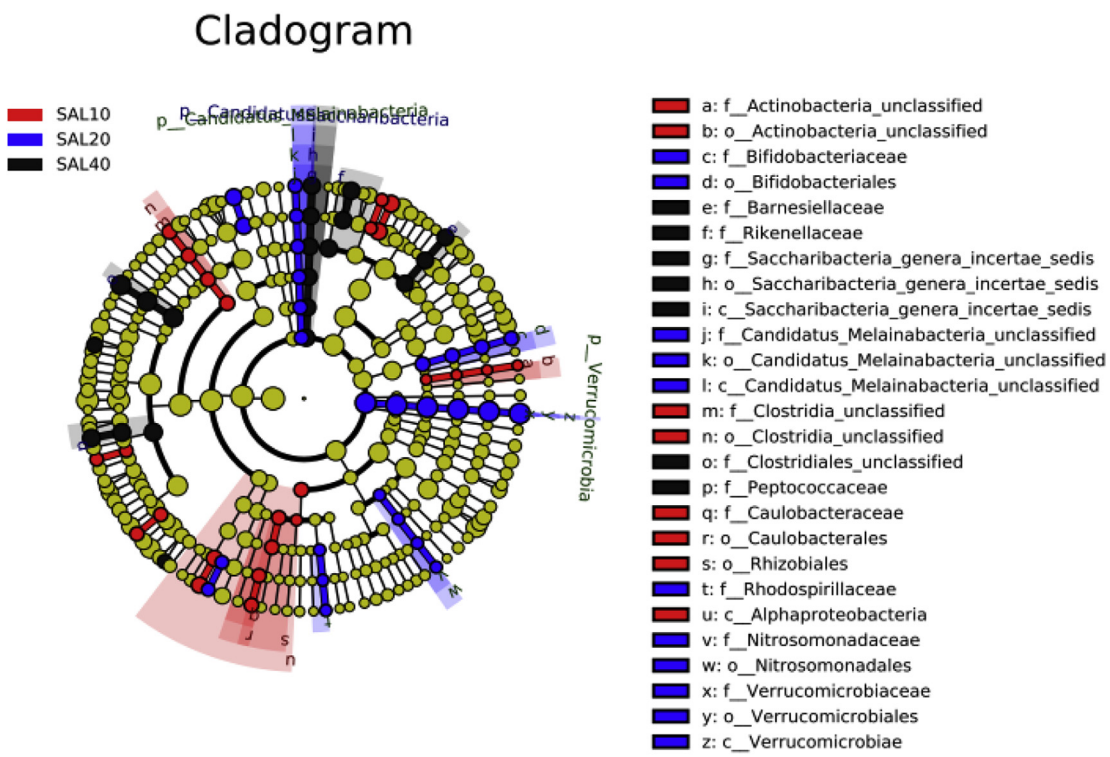

Fig. 4. LEfSe identified the most distinguishingly abundance of taxa in the gut microbiota from the furan-induced mouse model. Taxonomic cladogram obtained from LEfSe analysis of 16 S rDNA sequencing. (Red) SAL 10 enriched taxa; (Blue) SAL 20 enriched taxa; (Black) SAL 40 enriched taxa. The brightness of each dot is positive correlated with its effect size. (For interpretation of the references to colour in this figure legend, the reader is referred to the Web version of this article.)

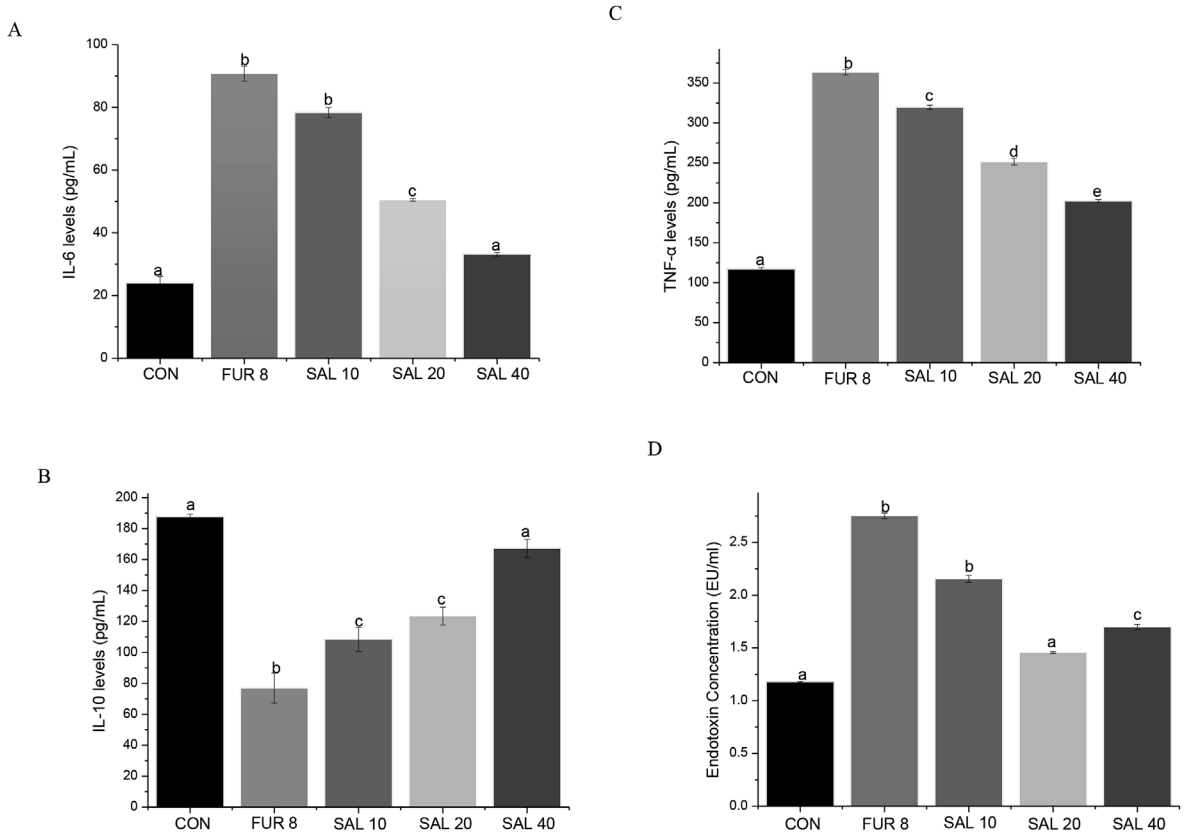

Fig. 5. Effects of SAL on the levels of IL-6, IL-10, TNF-α, and LPS content in the serum of furan-treated mice. (A) IL-6; (B) IL-10; (C) TNF-α; (D) LPS. All values are expressed as means ± standard deviation. The same superscript upper case letters indicates that there is no significant differences in data between the groups which have the same superscript letters ($p > 0.05$). Different superscript letters indicates statistically significant differences between the groups whose superscript letters are different ($p < 0.05$).

anti-obesity effects (Shen et al., 2017), and interfering immunologic and metabolic function (Dao et al., 2016), and their levels corresponded with serum LPS contents. *Roseburia*, known as a butyric acid producer, have a strong xylanase activity (Chassard et al., 2010). Thus, gut microbiota was more inclined to SAL 20 than the other groups, which may be conductive to stimulate the growth of gut bacteria *Akkermansia* and *Roseburia*. At the same time, when mice were supplied with SAL, the growth of pathogenic bacteria such as *Blautia*, *Desulfovibrio* and *Sporobacter* were significantly suppressed. And *Blautia* could exist extensively in NAFLD patients (Qin et al., 2014). Our results clearly demonstrated that SAL supplementation played an ameliorative role in liver injury partially through modulating gut microbiota.

Cytokines are associated with immune response, inflammation, and tissue damage or repair. Intestinal bacteria contribute to activating relevant mechanisms and subsequently triggering an inflammatory adaptive immune response that involves several cytokines, such as IL-1, IL-2, IL-6, IL-10, IL-22, and TNF-α (Decicco et al., 1998). The generated immune response also has direct impact on intrahepatic immune responses. For example, IL-6 is an effective activator of hepatic signal transducers and activators of transcription 3 (STAT3) pathway and is diffusely featured as a participator in different facets of liver pathophysiology, including hepatic regeneration (Sakamoto et al., 1999), induction of the acute phase response (Hirano, 1998) and bile tract diseases and wound healing (Demetris et al., 2006). It also generally acts as a proinflammatory cytokine for the reason that it is heightened together with other proinflammatory cytokines such as TNF-α and IL-1 in the course of early phases of inflammatory responses (Xing et al., 1998). Expression of TNF-α can stimulate NFκB pathways and cause damage to cells (Bian et al., 2017). It has been presumed that anti-inflammatory cytokines such as TGF-β and IL-10 are crucial inhibitors of liver DC maturation (Crispe et al., 2010). Our data about IL-6, IL-10 and TNF-α demonstrated that furan activated inflammatory cells and magnified the inflammatory response by releasing various cytokines. However, SAL replenishment prominently reduced the contents of pro-inflammatory cytokines including TNF-α and IL-6 and enhanced the content of anti-inflammatory cytokine IL-10 in the systematic circulation.

Systemic low-grade inflammation is mainly attributed to the increment of plasma endotoxins, particularly LPS. For instance, gut microbiota-derived LPS is considered as a crucial factor in liver disease by activating IL-6/STAT3 signaling. Because of activated liver IL-6/STAT3 signaling, hepatic DCs need a higher threshold to maturation-inducing stimuli (Lunz et al., 2007). Simultaneously, LPS activates innate immune cells, such as macrophages, by acting as a ligand for toll-like receptor 4 and triggers the inflammatory response (Zhou et al., 2018). Treatment with SAL at 10, 20 and 40 mg/kg/day could suppress the enhancement of LPS level contrasted with the furan-treated group (Fig. 5D), implying that LPS acted a pivotal role between intestinal microbiota and host inflammation, and SAL prevented intestinal LPS-relative microbiota dysbiosis by reducing LPS content and further inhibited systemic low-grade inflammation. Importantly, the content of LPS in SAL 20 was significantly decreased compared to the FUR 8 group, in conformity to the decline in LPS-producing genera and the increase in LPS-suppressing genera, which indicated that SAL reduced the serum LPS level not in a dose-dependent manner. Related research showed SAL could directly restrain the survival and proliferation of intestinal epithelial cells in a dose and time-dependent manner, low doses of SAL performed lower cytotoxicity (Wang et al., 2019). Considering the dose of SAL intake, there is evidence that SAL 20 can set up a structurally balanced conformation of the gut microbiota that may unleash a health benefit to the host by reducing the level of LPS. Thus, a better comprehension of the effects of SAL on modulating gut microbiota would be significant.

For further investigation of the effects of SAL on the regulation of gut microbiota, we discerned the specific bacterial taxa related with the treatment of SAL by LEfSe. Specific and significant enhancement of *Verrucomicrobia* mainly depends on the growth of *Akkermansia*, which plays a role during liver injury progressions (Shen et al., 2017). *Akkermansia* was crucial for decreasing systemic low-grade inflammation, and SAL obviously increased *Akkermansia*, which reduced LPS contents and pro-inflammatory cytokines, and ultimately prevented inflammation. In view of previous studies, the results showed that SAL treatment could alleviate liver diseases by changing the composition of gut microbiota, and certain genera attached to 2 primary phyla, *Verrucomicrobia* and *Actinobacteria*, which act as biomarkers.

In summary, we pioneeringly revealed that the administration of SAL alleviated liver injury induced by furan, as well as maintained the balance of gut microbiota. Studies performed with 16 S rDNA have proved that SAL could upregulate LPS-suppressing genera and downregulate LPS-producing genera, both of which interacted with signaling pathways involved in the progress of liver injury. Exploring these signaling pathways helps further elucidate the medicinal value of SAL in the prevention of furan toxicity. Relevant metabonomics methods will be applied to explore how specific metabolic pathways are modified.

Conflicts of interest

The authors declare that there is no conflict of interest.

Abbreviations used

ANOVA, analysis of variance; ALT, glutamic-pyruvic transaminase; AST, aspartate transaminase; ELISA, enzyme-linked immunosorbent assay; GSH, glutathione; GST, glutathione S-transferase; HCC, alcoholic liver disease and hepatocellular carcinoma; HE, hematoxylin-eosin staining; IARC, International Agency for Research on Cancer; IL-6, interleukin- 6; IL-10, interleukin-10; LDA, the linear discriminant analysis; LEfSe, linear discriminant analysis effect size; LPS, Lipopolysaccharides; MC-LR, Microcystins-LR; MDA, malondialdehyde; NAFLD, non-alcoholic fatty liver disease; NASH, non-alcoholic steatohepatitis; OTUs, operational taxonomic units; PCoA, principal co-ordinates analysis; SAL, salidroside; SOD, superoxide dismutase; STAT3, signal transducers and activators of transcription 3; TNF-α, tumor necrosis factor α.

Acknowledgements

This work was supported by funds from the National Natural Science Foundation of China (No. 31471666, 31571939). The authors gratefully acknowledge the fund supports.

Transparency document

Transparency document related to this article can be found online at https://doi.org/10.1016/j.fct.2019.01.007.

References

Bakhiya, N., Appel, K.E., 2010. Toxicity and carcinogenicity of furan in human diet. Arch. Toxicol. 84, 563–578.
Bian, X., Tu, P., Chi, L., Gao, B., Ru, H., Lu, K., 2017. Saccharin induced liver inflammation in mice by altering the gut microbiota and its metabolic functions. Food Chem. Toxicol. 107, 530–539.
Bittencourtoliveira, M., Hereman, T., Macedosilva, I., Dias, C., Sasaki, F., Moura, A., 2014. Phytotoxicity associated to microcystins: a review. Braz. J. Biol. 74, 753–760.
Caesar, R., Tremaroli, V., Kovatchevadatchary, P., Cani, P.D., Bäckhed, F., 2015. Crosstalk between gut microbiota and dietary lipids aggravates WAT inflammation through TLR signaling. Cell Metabol. 22, 658–668.
Carvalho, F.A., Koren, O., Goodrich, J.K., Johansson, M.E., Nalbantoglu, I., Aitken, J.D., Su, Y., Chassaing, B., Walters, W.A., González, A., 2012. Transient inability to manage proteobacteria promotes chronic gut inflammation in TLR5-deficient mice. Cell Host Microbe 12, 139–152.
Chang, C.J., Lin, C.S., Lu, C.C., Martel, J., Ko, Y.F., Ojcius, D.M., Tseng, S.F., Wu, T.R., Chen, Y.Y.M., Young, J.D., 2015. Corrigendum: ganoderma lucidum reduces obesity in mice by modulating the composition of the gut microbiota. Nat. Commun. 6, 7489.
Chassard, C., Goumy, V., Leclerc, M., Del'Homme, C., Bernalier-Donadille, A., 2010.

Characterization of the xylan-degrading microbial community from human faeces. FEMS Microbiol. Ecol. 61, 121–131.
Clemente, J.C., Ursell, L.K., Parfrey, L.W., Knight, R., 2012. The impact of the gut microbiota on human health: an integrative view. Cell 148, 1258–1270.
Condurso, C., Cincotta, F., Verzera, A., 2018. Determination of furan and furan derivatives in baby food. Food Chem. 250, 155–161.
Cordelli, E., Leopardi, P., Villani, P., Marcon, F., Macrì, C., Caiola, S., Siniscalchi, E., Conti, L., Eleuteri, P., Malchiodi-Albedi, F., 2010. Toxic and genotoxic effects of oral administration of furan in mouse liver. Mutagenesis 25, 305–314.
Crews, C., Castle, L., 2007. The determination of furan in foods - challenges and solutions. LC-GC Eur. 20, 498–503.
Crispe, I.N., Giannandrea, M., Klein, I., John, B., Sampson, B., Wuensch, S., 2010. Cellular and molecular mechanisms of liver tolerance. Immunol. Rev. 213, 101–118.
Dao, M.C., Everard, A., Aronwisnewsky, J., Sokolovska, N., Prifti, E., Verger, E.O., Kayser, B.D., Levenez, F., Chilloux, J., Hoyles, L., 2016. Akkermansia muciniphila and improved metabolic health during a dietary intervention in obesity: relationship with gut microbiome richness and ecology. Gut 65, 426–436.
De, M.S., Rychlicki, C., Agostinelli, L., Saccomanno, S., Candelaresi, C., Trozzi, L., Mingarelli, E., Facinelli, B., Magi, G., Palmieri, C., 2014. Dysbiosis contributes to fibrogenesis in the course of chronic liver injury in mice. Hepatology 59, 1738–1749.
Decicco, L., Rikans, L., Tutor, C., Hornbrook, K., 1998. Serum and liver concentrations of tumor necrosis factor alpha and interleukin-1beta following administration of carbon tetrachloride to male rats. Toxicol. Lett. 98, 115–121.
Demetris, A.J., Specht, S., Nozaki, I., 2006. Biliary wound healing, ductular reactions, and IL-6/gp130 signaling in the development of liver disease. World J. Gastroenterol. 12, 3512–3522.
Endale, M., Park, S.C., Kim, S., Kim, S.H., Yang, Y., Cho, J.Y., Rhee, M.H., 2013. Quercetin disrupts tyrosine-phosphorylated phosphatidylinositol 3-kinase and myeloid differentiation factor-88 association, and inhibits MAPK/AP-1 and IKK/NF-κB-induced inflammatory mediators production in RAW 264.7 cells. Immunobiology 218, 1452–1467.
Henaomejia, J., Elinav, E., Jin, C., Hao, L., Mehal, W.Z., Strowig, T., Thaiss, C.A., Kau, A.L., Eisenbarth, S.C., Jurczak, M.J., 2012. Inflammasome-mediated dysbiosis regulates progression of NAFLD and obesity. Nature 482, 179–185.
Hirano, T., 1998. Interleukin 6 and its receptor: ten years later. Int. Rev. Immunol. 16, 249–284.
Hu, G., Zhu, Y., Hernandez, M., Koutchma, T., Shao, S., 2016. An efficient method for the simultaneous determination of furan, 2-methylfuran and 2-pentylfuran in fruit juices by headspace solid phase microextraction and gas chromatography-flame ionisation detector. Food Chem. 192, 9–14.
Ito, E., Kondo, F., Harada, K., 2001. Intratracheal administration of microcystin-LR, and its distribution. Toxicon 39, 265–271.
Jayaraj, R., Anand, T., Rao, P.V., 2006. Activity and gene expression profile of certain antioxidant enzymes to microcystin-LR induced oxidative stress in mice. Toxicology 220, 136–146.
Li, J., Li, R., Li, J., 2017. Current research scenario for microcystins biodegradation - a review on fundamental knowledge, application prospects and challenges. Sci. Total Environ. 595, 615–632.
Louis, P., Young, P., Holtrop, G., Flint, H.J., 2010. Diversity of human colonic butyrate-producing bacteria revealed by analysis of the butyryl-CoA: acetate CoA-transferase gene. Environ. Microbiol. 12, 304–314.
Lunz III, J.G., Specht, S.A., Murase, N., Isse, K., Demetris, A.J., 2007. Gut-derived commensal bacterial products inhibit liver dendritic cell maturation by stimulating hepatic interleukin-6/signal transducer and activator of transcription 3 activity. Pathobiology 46 (6), 1946–1959.
Maga, J.A., 1979. Furans in foods. CRC Crit. Rev. Food Technol 11, 355–400.
Martín, R., Chain, F., Miquel, S., Lu, J., Gratadoux, J.J., Sokol, H., Verdu, E.F., Bercik, P., Bermúdezhumarán, L.G., Langella, P., 2014. The commensal bacterium Faecalibacterium prausnitzii is protective in DNBS-induced chronic moderate and severe colitis models. Inflamm. Bowel Dis. 20, 417–430.
Pabst, M.J., Habig, W.H., Jakoby, W.B., 1974. Glutathione S-transferase A. A novel kinetic mechanism in which the major reaction pathway depends on substrate concentration. J. Biol. Chem. 249, 7140–7147.
Qin, N., Yang, F., Li, A., Prifti, E., Chen, Y., Shao, L., Guo, J., Le, C.E., Yao, J., Wu, L., 2014. Alterations of the human gut microbiome in liver cirrhosis. Nature 513, 59–64.
Sakamoto, T., Liu, Z., Murase, N., Ezure, T., Yokomuro, S., Poli, V., Anthony, J.D.M.D., 1999. Mitosis and apoptosis in the liver of interleukin-6–deficient mice after partial hepatectomy. Hepatology 29, 403–411.
Selmanoğlu, G., Karacaoğlu, E., Kiliç, A., Koçkaya, E.A., Akay, M.T., 2012. Toxicity of food contaminant furan on liver and kidney of growing male rats. Environ. Toxicol. 27, 613–622.
Shen, W., Shen, M., Zhao, X., Zhu, H., Yang, Y., Lu, S., Tan, Y., Li, G., Li, M., Wang, J., 2017. Anti-obesity effect of capsaicin in mice fed with high-fat diet is associated with an increase in population of the gut Bacterium *Akkermansia muciniphila*. Front. Microbiol. 8, 272.
Smith, C.J., Perfetti, T.A., Rumple, M.A., Rodgman, A., Doolittle, D.J., 2000. IARC group 2A Carcinogens" reported in cigarette mainstream smoke. Food Chem. Toxicol. 39, 183–205.
Walker, A.W., Sanderson, J.D., Churcher, C., Parkes, G.C., Hudspith, B.N., Rayment, N., Brostoff, J., Parkhill, J., Dougan, G., Petrovska, L., 2011. High-throughput clone library analysis of the mucosa-associated microbiota reveals dysbiosis and differences between inflamed and non-inflamed regions of the intestine in inflammatory bowel disease. BMC Microbiol. 11, 1–12.
Walters, W., Hyde, E.R., Berg-Lyons, D., Ackermann, G., Humphrey, G., Parada, A., Gilbert, J.A., Jansson, J.K., Caporaso, J.G., Fuhrman, J.A., 2016. Improved bacterial 16S rRNA gene (V4 and V4-5) and fungal internal transcribed spacer marker gene primers for microbial community surveys. mSystems 1, e00009–00015.
Wang, J.W., Pan, Y.B., Cao, Y.Q., Zhou, W., Lu, J.G., 2019. Salidroside regulates the expressions of IL-6 and defensins in LPS-activated intestinal epithelial cells through NF-κB/MAPK and STAT3 pathways. Iranian Journal of Basic Medical Sciences 22, 31–37.
X, C, A, D, H, Z, J, G, 2013. Neuroprotective effect of 2-(4-methoxyphenyl)ethyl-2-acetamido-2-deoxy-β-D-pyranoside against sodium nitroprusside-induced neurotoxicity in HT22 cells. Molecular\s&\scellular Biochemistry 383, 149–159.
Xing, Z., Gauldie, J., Cox, G., Baumann, H., Jordana, M., Lei, X.F., Achong, M.K., 1998. IL-6 is an antiinflammatory cytokine required for controlling local or systemic acute inflammatory responses. Journal of Clinical Investigation 101, 311–320.
Yang, Z.R., Wang, H.F., Zuo, T.C., Guan, L.L., Dai, N., 2016. Salidroside alleviates oxidative stress in the liver with non- alcoholic steatohepatitis in rats. Bmc Pharmacology & Toxicology 17, 16.
Yuan, Y., Wu, S.J., Liu, X., Zhang, L.L., 2013. Antioxidant effect of salidroside and its protective effect against furan-induced hepatocyte damage in mice. Food & Function 4, 763–769.
Zhang, L., Yu, H., Zhao, X., Lin, X., Tan, C., Cao, G., Wang, Z., 2010. Neuroprotective effects of salidroside against beta-amyloid-induced oxidative stress in SH-SY5Y human neuroblastoma cells. Neurochemistry International 57, 547–555.
Zhou, X.L., Yan, B.B., Xiao, Y., Zhou, Y.M., Liu, T.Y., 2018. Tartary buckwheat protein prevented dyslipidemia in high-fat diet-fed mice associated with gut microbiota changes. Food and Chemical Toxicology 119, 296–301.
Zou, H., Liu, X., Han, T., Hu, D., Wang, Y., Yuan, Y., Gu, J., Bian, J., Zhu, J., Liu, Z.P., 2015. Salidroside protects against cadmium-induced hepatotoxicity in rats via GJIC and MAPK pathways. Plos One 10, e0129788.
Zuckerman, J.A., 1995. IARC monographs on the evaluation of carcinogenic risks to humans. Journal of Clinical Pathology 48, 691.